Cell Metabolism
Article

BBS-Induced Ciliary Defect Enhances Adipogenesis, Causing Paradoxical Higher-Insulin Sensitivity, Glucose Usage, and Decreased Inflammatory Response

Vincent Marion,[1,*] Anaïs Mockel,[1] Charlie De Melo,[1] Cathy Obringer,[1] Aurélie Claussmann,[1] Alban Simon,[2] Nadia Messaddeq,[3] Myriam Durand,[4] Luc Dupuis,[5] Jean-Philippe Loeffler,[5] Peter King,[6] Catherine Mutter-Schmidt,[2] Nikolai Petrovsky,[7] Corinne Stoetzel,[1] and Hélène Dollfus[1,4]

[1]Laboratoire de Physiopathologie des syndromes rares héréditaires, AVENIR-Inserm, EA3949, Université de Strasbourg, 11 rue Humann, 67085 Strasbourg, France
[2]Inserm, Centre d'Investigation Clinique de Strasbourg, CIC-P 1002, CHRU de Strasbourg, F67091 Strasbourg, France
[3]Institut de Génétique et de Biologie Moléculaire et Cellulaire de Strasbourg Inserm U596, CNRS, UMR7104; Université de Strasbourg, Ilkirch, F-67400 France
[4]Service de Génétique Médicale, Hôpitaux Universitaires de Strasbourg, France
[5]Inserm U692, Laboratoire de Signalisations Moléculaires et Neurodégénérescence, Strasbourg, F-67085 France
[6]William Harvey Research Institute, Queen Mary University of London, London EC1M 6BQ, UK
[7]Flinders Medical Centre/Flinders University, Bedford Park, Australia 5042
*Correspondence: vincent.marion@unistra.fr
http://dx.doi.org/10.1016/j.cmet.2012.08.005

SUMMARY

Studying ciliopathies, like the Bardet-Biedl syndrome (BBS), allow the identification of signaling pathways potentially involved in common diseases, sharing phenotypic features like obesity or type 2 diabetes. Given the close association between obesity and insulin resistance, obese BBS patients would be expected to be insulin resistant. Surprisingly, we found that a majority of obese BBS patients retained normal glucose tolerance and insulin sensitivity. Patient's adipose tissue biopsies revealed upregulation of adipogenic genes and decrease of inflammatory mediators. In vitro studies on human primary mesenchymal stem cells (MSCs) showed that BBS12 inactivation facilitated adipogenesis, increased insulin sensitivity, and glucose utilization. We generated a *Bbs12*$^{-/-}$ mouse model to assess the impact of Bbs12 inactivation on adipocyte biology. Despite increased obesity, glucose tolerance was increased with specific enhanced insulin sensitivity in the fat. This correlated with an active recruitment of MSCs resulting in adipose tissue hyperplasia and decreased in inflammation.

INTRODUCTION

Better understanding of the molecular mechanisms underlying obesity-associated type 2 diabetes mellitus (T2DM) is a high research priority in view of the global obesity pandemic. Many therapeutic approaches have been developed to help reduce obesity and T2DM, including peroxisome proliferator-activated receptors (PPAR)-γ agonists, cannabinoid receptor antagonists, and serotonin uptake inhibitors (Berger et al., 1996; Kast-Woelbern et al., 2004; Spiegelman, 1998), but unfortunately many of these treatments including rosiglitazone, rimonabant, and sibutramine have been subsequently withdrawn from use due to side effects (Kohlroser et al., 2000; Scheen, 2001). There is consequently a major unmet need for new therapies for the rapidly growing population of patients with obesity and T2DM. Rare genetic disorders have emerged as valuable models for discovering new pieces of the jigsaw on the origins of obesity and insulin resistance leading to T2DM (Nachury et al., 2007). Ciliopathies are a group of inherited monogenic syndromes due to a defect in the primary cilium, an ubiquitously distributed organelle implicated in the detection, transmission, and interpretation of various types of intracellular and extracellular signals (Hildebrandt et al., 2011; Mok et al., 2010; Satir et al., 2010; Sen Gupta et al., 2009; Cardenas-Rodriguez and Badano, 2009; Girard and Petrovsky, 2011; Mockel et al., 2011; Novarino et al., 2011). Interestingly, several of the ciliopathies including the Bardet Biedl syndrome (BBS) and Alstrom syndrome are associated with morbid obesity and diabetes. BBS is genetically heterogeneous ciliopathy, with 17 BBS genes identified so far, but with a cardinal clinical trait of all BBS types being severe obesity (Généreux et al., 2011; Sheffield, 2010; Zaghloul and Katsanis, 2009). BBS-induced obesity has previously been proposed to be due to the incapacity of the hypothalamus to respond to leptin (Rahmouni et al., 2008a), the appetite-controlling hormone synthesized and secreted by adipose tissue. This effect was ascribed to a failure of the transport of the leptin receptor to the primary cilium (Seo et al., 2009) of hypothalamic neurons resulting in hyperphagia, as observed in various BBS knockout mouse models and described in human case reports (Berbari et al., 2008). We previously demonstrated that the differentiating preadipocyte is transiently ciliated (Marion et al., 2009), associated with a peak expression of the different BBS proteins (Forti et al., 2007). In vitro BBS inactivation during adipocyte differentiation resulted in enhanced adipogenesis through repression of antiadipogenic signaling pathways including the Wnt cascade, combined with activation of proadipogenic pathways through increased expression of PPARγ, highlighting the role of BBS

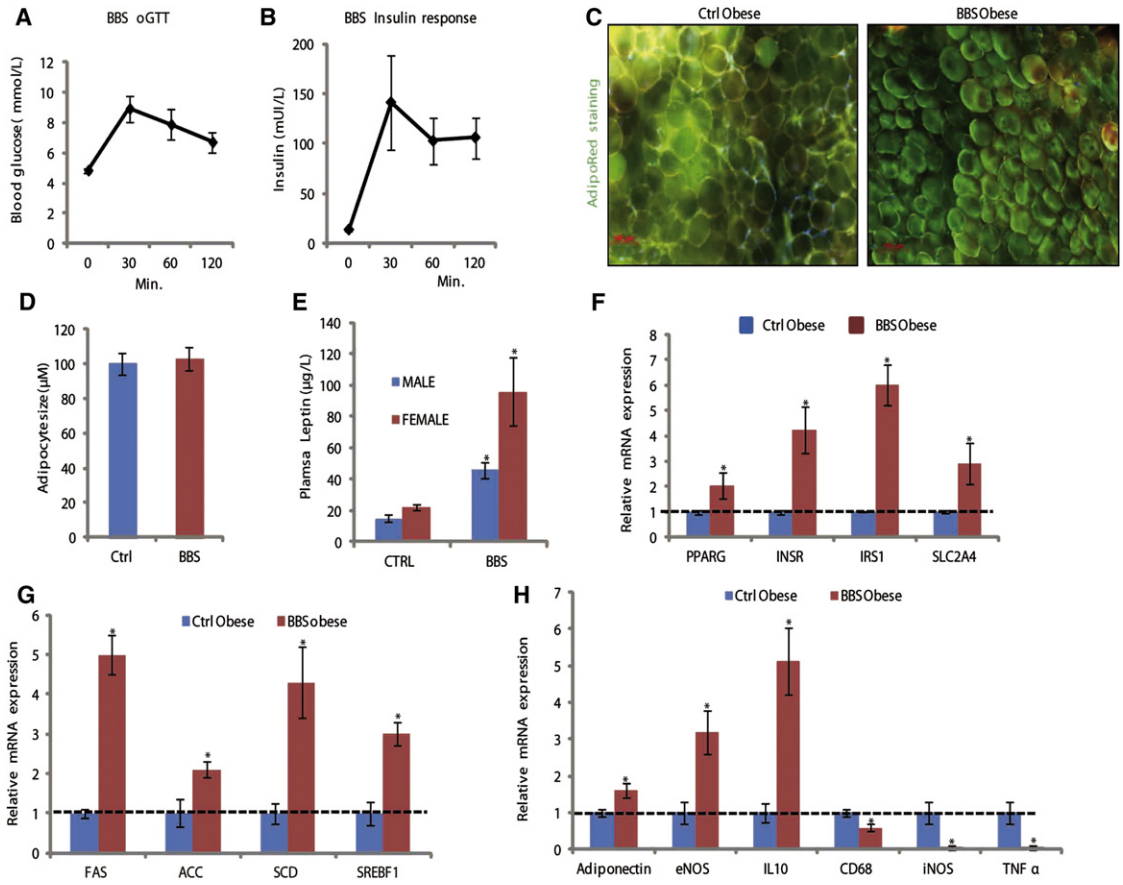

Figure 1. Human BBS Adipose Tissue Phenotype

(A) Glucose tolerance test in BBS obese patients (BMI >30 kg/m^2).

(B) Insulin response curve to glucose administration in the corresponding BBS patients.

(C) Pictures of AdipoRed-stained subcutaneous adipocytes from the corresponding BBS patients.

(D) Adipocyte cell size in corresponding subcutaneous adipose tissue ($\geq$200 cells per patient).

(E) Circulating Leptin concentration in the corresponding BBS patients.

(F) Relative mRNA levels in the subcutaneous adipose tissue of the corresponding BBS patients.

(G) Adipogenic gene-expression levels in subcutaneous WAT in the subcutaneous adipose tissue of the corresponding BBS patients.

(H) Inflammatory-related gene-expression levels in the subcutaneous adipose tissue of the corresponding BBS patients.

Values are expressed as mean ± SEM; n = 6–8 patients in (A)–(E); n = 4 in (F), (G), and (H); *p < 0.05. See also Table S2.

proteins in the regulation of adipogenesis. Interestingly, a recent metabolic study carried on 50 young (average age ~15 years) BBS patients and 100 obese BMI-matched controls made the surprising finding that obese BBS patients had, despite greater visceral adiposity, better glucose tolerance and lower glycosylated hemoglobin than obese non-BBS controls (Feuillan et al., 2011), suggesting that BBS gene mutations have a positive effect on glucose regulation despite inducing visceral adiposity. Given the tight link between visceral adiposity and insulin resistance in all other forms of obesity, we wished to understand how in the presence of obesity and hyperleptinaemia BBS patients are able to avoid insulin resistance and maintain normoglycemia with the hope that this could lead to therapeutic strategies to reverse obesity-associated T2DM. In particular, we wished to test the hypothesis that the BBS proteins play a key role in regulation of adipocyte differentiation, and interruption of BBS signaling disinhibits adipocyte generation leading to increased adipocyte insulin sensitivity with a lack of low-grade inflammation, which thereby provides a glucose sink in adipose tissue.

RESULTS

Phenotype of Human BBS Fat Tissue

Obesity is a cardinal clinical feature of BBS (Beales, 2005). To characterize this phenotype, we performed oral glucose tolerance tests (oGTT) and plasma insulin and leptin profiles on a group of obese adult subjects (n = 16, mean age ~27 years and mean BMI >30 kg/m^2) with identified BBS mutations (Table S1 for list of mutated patients). The subjects with BBS had a mean fasting blood glucose pre-oGTT of 4.85 mmol/L, which increased to a mean of 6.71 mmol/L at 120 min after glucose ingestion. Thus, according to the 1999 WHO criteria for interpretation of oGTT results, obese BBS subjects were not glucose intolerant (Figure 1A). The plasma insulin profile during the oGTT also remained within the normal range (Figure 1B). Subsequent analysis

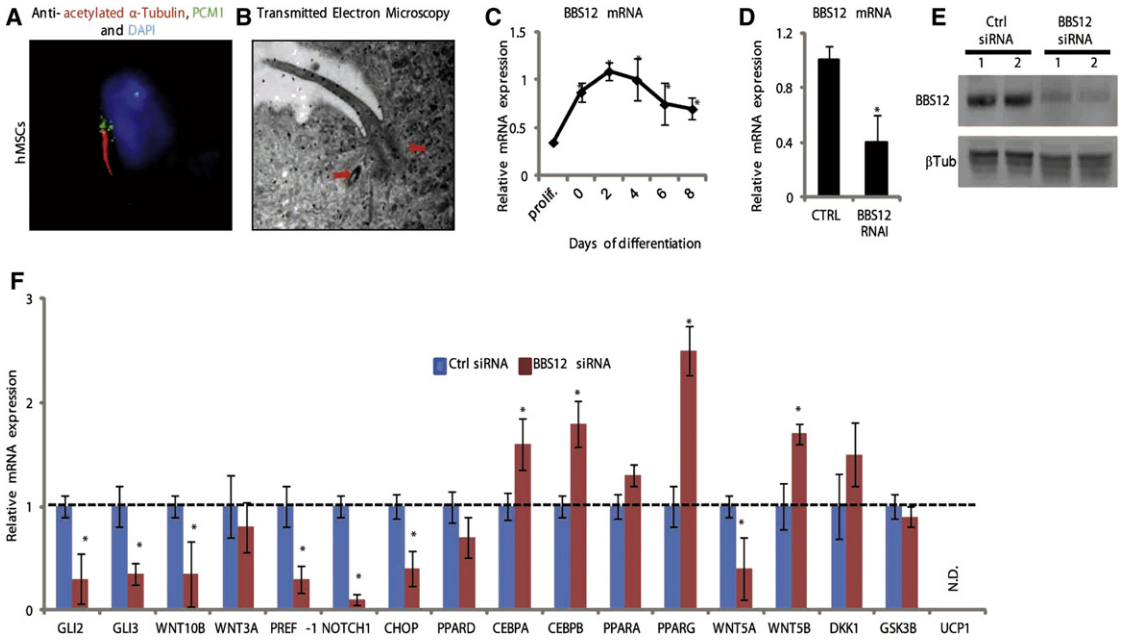

Figure 2. Bbs12 Depletion Represses Antiadipogenic Pathways Hence Favoring Adipogenesis

(A) Primary cilium (red) detected in hMSCs at day 4 of adipogenic differentiation with surrounding pericentriolar material (green).

(B) Centrioles (arrows) detected at the base of the primary cilium at day 4 of adipogenic differentiation.

(C) Relative mRNA levels of BBS12 during adipogenic differentiation of hMSCs.

(D) Relative mRNA levels of BBS12 in hMSCs at D4 of adipogenic differentiation.

(E) Immunodetection of BBS12 with corresponding β-tubulin immunodetection as loading control.

(F) Relative mRNA levels of adipogenic regulatory genes at D4 of adipogenic differentiation.

Values are expressed as mean ± SEM; n = 4 in (C), (D), (E), and (F); *p < 0.05 for differentiation versus proliferation levels in (C) and CTRLsiRNA versus BBS12siRNA in (D) and (E). See also Table S1 and Figure S1.

on deep subcutaneous adipose tissue biopsies from obese BBS patients and controls with comparable BMI (>30 kg/m^2) demonstrated similar adipocyte cell size with a mean diameter of 100 μm (Figures 1C and 1D). Characteristic hyperleptinemia was also found in the BBS patients (Figure 1E) Gene-expression analysis of adipose tissue from subjects with BBS (Figure 1F) demonstrated increased expression of key genes involved in insulin signaling pathways including the insulin receptor (INSR), insulin receptor substrate 1 (IRS1), and glucose transporter 4 (SLC2A4). Similarly, the expression of PPARγ and downstream adipogenic PPARγ response genes, *FAS, ACC, SCD2*, and *SREBP1c* were all increased in BBS adipose tissue (Figure 1G). Obesity gives rise to a state of chronic, low-grade inflammation associated with infiltration of macrophages (Greenberg and Obin, 2006; Shoelson et al., 2006a). Anti-inflammatory and antidiabetic Adiponectin, endothelial nitric oxide synthase (eNOS), and Interleukin10 gene expression were found upregulated in the BBS adipose tissue. This correlated with lower levels of marcrophage marker CD68 and proinflammatory mediators such as inducible nitric oxide (iNOS) and tumor necrosis factor alpha (TNFα) in the BBS obese patients' adipose tissue highlighting an absence of inflammation.

Inactivation of BBS12 in hMSCs Favors Adipogenic Differentiation

To understand the basis for this upregulated insulin signaling pathway gene-expression profile in human BBS adipose tissue, we studied adipocyte differentiation using human mesenchymal stem cells (hMSCs), adipocyte precursors, originating from the bone marrow (Cristancho and Lazar, 2011; Slagman et al., 2011) among which ciliated cells could be detected (Figures S1A and S1B). On day 4 of adipogenic differentiation, transient primary cilia were observed on the differentiating hMSCs (Figure 2A), with the characteristic feature of centrioles at their basal body (arrows; Figure 2B, right picture). Concomitant to this transient ciliated status, BBS12 mRNA expression levels peaked (Figure 2C) (as did the transcript levels of other interacting chaperone BBS proteins; BBS10 and BBS6 (Seo et al., 2010) (Figure S1C). siRNA-mediated knockdown of any of the three interacting chaperone BBS proteins resulted in a significant decrease in the number of ciliated cells indicating these BBS proteins are required during adipogenic differentiation of hMSCs (Figures 2D, 2E, S1D, and S1E).

To assess the involvement of BBS12 expression for adipogenic differentiation of hMSC, we performed siRNA-mediated knock down of *BBS12* on hMSC and then measured the expression of regulatory adipogenic genes at differentiation day 4 (corresponding to 5 days post-siRNA treatment) (Figure 2D). Significantly reduced expression levels of Hedgehog (*GLI2*, *GLI3*), Wnt (Laudes, 2011; Taipaleenmäki et al., 2011) (*Wnt10B*), and Notch (*NOTCH1*) signaling pathways as well as the transcription factor CHOP (Batchvarova et al., 1995) were observed in BBS12-depleted hMSCs (Figure 2E), indicating repression of antiadipogenic pathways. At the same time,

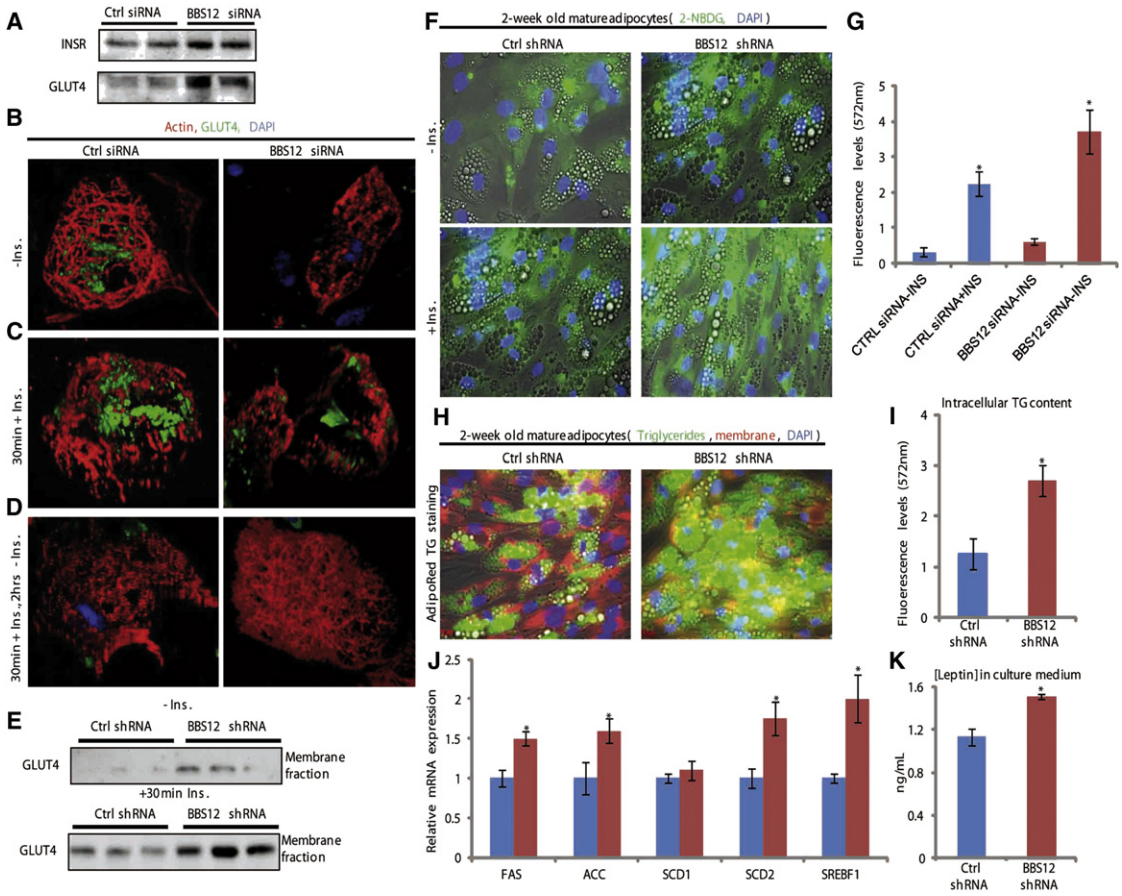

Figure 3. Increase Glucose Absorption Capacity in BBS12-Deprived Adipocytes

(A) Immunodetection IR and GLUT4 on cell lysates from 1-week-old mature human adipocytes.

(B–D) 3D representation of mature adipocytes showing the effect of Ins. on actin mesh (red) and GLUT4 localization (green).

(E) Glut4 membrane content upon Ins. stimulation.

(F) 2-NBDG absorption with ±Ins. stimulation.

(G) Fluorescent quantification of intracellular 2-NBDG in adipocytes ±Ins. stimulation.

(H) AdipoRed staining of intracellular triglycerides (TG) in green and plasma membrane stained with Image-iT (red).

(I) Fluorescent quantification of the corresponding intracellular TG content.

(J) Adipogenic gene expression levels in 2-week-old mature adipocytes.

(K) Leptin concentration in 4 days conditioned adipocyte culture medium from 3-week-old primary mature adipocytes

Values are expressed as mean ± SEM, n = 8 in (G) and (I); n = 4 in (K) and (L); *$p < 0.05$ for CTRL siRNA versus BBS12 siRNA. See also Table S3 and Figure S2.

expression levels of the proadipogenic genes *CEBPA*, *CEBPB*, *PPARG*, *WNT5B*, and *DKK1* were significantly increased, hence favoring hMSC adipogenesis. Collectively, these results show that BBS12 inactivation favors adipogenesis in hMSCs by repressing antiadipogenic signaling cascades.

BBS12 Inactivation Increases Glucose Absorption by Mature Human Adipocytes

PPARγ expression improves insulin sensitivity and increases glucose uptake in mature adipocytes (Chiarelli and Di Marzio, 2008; Choi et al., 2011) by regulating genes involved in glucose metabolism. Following BBS12 inactivation in hMSC, we observed significantly increased expression of the insulin receptor (IR) and GLUT4 protein levels (Figures 3A, S2A, and S2B). We next tested whether BBS12 inactivation impacted on IR and GLUT4 cellular dynamics in response to insulin stimulation. In the absence of insulin, the IR and GLUT4 were located at the cell periphery and inside an intracellular compartment, respectively (de Foresta et al., 2011) (Figure S2C). GLUT4 was localized below an intact actin mesh (Figures 3B and S2D, –Ins.). In response to insulin treatment for 30 min, again irrespective of BS12 expression, the actin mesh was disorganized and GLUT4 was targeted to the cell membrane (Figures 3C and S2D; 30 min Ins.). GLUT4 recycling was also unaffected in absence of BBS12 as 2 hr after the removal of insulin, the actin network was restored and GLUT4 was recycled back inside the intracellular space (Figures 3D and S2D; 30 min Ins.; 2 hr –Ins.). However, the increased GLUT4 expression in BBS12-depleted adipocytes was associated with an increased GLUT4 plasma membrane content after insulin stimulation (Figures 3E and S2E). Importantly, the increased IR and GLUT4 expression levels and membrane targeting upon insulin stimulation in

BBS12-depleted adipocytes resulted in an increased glucose absorption capacity as measured by 1.5 fold higher absorption of the fluorescent glucose analog, 2-NBDG by BBS12-depleted adipocytes (Figures 3F and 3G).

BBS12 Depletion in Human Adipocytes Increases Insulin Sensitivity, Enhances Glucose Absorption, and Increases Intracellular Triglyceride Content

Having found an increased glucose absorption in BBS12-depleted adipocytes, we measured intracellular TG levels in 2-week-old mature adipocytes (Figure 3H) and found significantly higher TG content in BBS12-depleted adipocytes (Figure 3I), a feature previously described in adipocytes derived from BBS patients' dermal fibroblasts (Marion et al., 2009). To explain the increased TG content, we performed a comparative analysis of genes involved in fat metabolism in BBS12-depleted adipocytes. Expression levels of *FAS, ACC, SCD*, and *SREBF1* were upregulated in BBS12-depleted adipocytes (Figure 3J). In addition, leptin concentration in 4 day adipocyte-conditioned medium was higher for the BBS12-depleted 3-week-old mature adipocytes (Figure 3K).

The Bbs12 Knockout Mouse (*Bbs12*$^{-/-}$) Reproduces BBS Cardinal Clinical Features including Obesity

To unravel the pathophysiological implications underlying the above findings on human BBS-depleted adipocytes, we generated a Bbs12 knockout mouse (*Bbs12*$^{-/-}$) model using the approach depicted in Figures S3A and S3B. No Bbs12 expression could be measured in *Bbs12*$^{-/-}$ tissues as exemplified in the adipose tissues and the kidneys (Figure 4A). *Bbs12*$^{-/-}$ mice, although smaller at birth (Figure 4B), reached the weight of the WT control littermates at 8 week-old and finally became obese later in life. Food intake in mice of same weight (8 weeks of age) was significantly higher in *Bbs12*$^{-/-}$ mice (Figure 4C), whereas nocturnal energy expenditure was similar between the two groups (Figure S3C). At 12 weeks of age, the *Bbs12*$^{-/-}$ mice were clearly obese (Figure 4D) and presented retinal degeneration defined by a thinning of the outer nuclear layer (ONL) and the loss of the outer segment (OS) (Figure 4E). *Bbs12*$^{-/-}$ mice did not exhibit detectable structural renal abnormality like cystogenesis at 16 weeks of age (Figure S3D), unlike some other previously described BBS mouse models. Hyperleptinemia, a common trait in other BBS mouse models and human patients (Feuillan et al., 2011; Imhoff et al., 2011; Rahmouni et al., 2008a), was also present in *Bbs12*$^{-/-}$ mice (Figure 4F). Associated with the obese phenotype, *Bbs12*$^{-/-}$ epididymal fat deposits were 1.5 times bigger than wild-type (WT) littermates (Figure 4G) and the lipogenic proteins FAS and AceCS1 were increased in *Bbs12*$^{-/-}$ adipose tissue (Figures 4H and S3E).

Obese *Bbs12*$^{-/-}$ Mice Present Increased Insulin Sensitivity

To better understand the impact of BBS12-induced ciliary dysfunction on the fat biology, we measured fasting glucose and insulin levels in obese *Bbs12*$^{-/-}$ mice (~40 g body weight) and WT littermates (~30 g body weight) and found no significant differences (Figures 5A and 5B), thereby mimicking our findings. Interestingly, obese *Bbs12*$^{-/-}$ mice had lower peak glucose levels in the GTT than WT mice (Figure 5C). The corresponding plasma insulin in the first hour after glucose administration similarly showed no significant difference plasma insulin levels in the *Bbs12*$^{-/-}$ mice compared to the WT (Figure 5D). Consistent with absence of BBS12 conferring enhanced insulin sensitivity, the insulin tolerance test (ITT) that demonstrated an enhanced hypoglycemic response to injected insulin in the obese *Bbs12*$^{-/-}$ mice (Figure 5E). Overall, these data show that despite their obesity *Bbs12*$^{-/-}$ mice have enhanced rather than diminished insulin sensitivity.

BBS12-Deficient Adipocytes Have Enhanced Insulin Sensitivity and Glucose Absorption

The enhanced hypoglycemic response to insulin in *Bbs12*$^{-/-}$ mice could result from increased insulin sensitivity of other non-adipose insulin-responsive tissues, such as liver or muscle. To assess whether the effect of BBS12 inactivation on insulin sensitivity was tissue specific, we injected insulin (5U/kg body weight) into fasted mice and 30 min later harvested the liver, muscle, and visceral adipose tissue. Insulin-mediated phosphorylation of AKT on serine 473 (p-AKT) was significantly increased in *Bbs12*$^{-/-}$ adipose tissues but not in liver or muscle, suggesting that the increased insulin sensitivity of *Bbs12*$^{-/-}$ mice was predominantly localized to adipose tissue (Figures 5F–5H). To confirm this finding, we measured p-AKT levels in isolated primary adipocytes in response to insulin stimulation and found BBS12-depleted adipocytes had double the amount p-AKT (Figures 5I and S4). Increased p-AKT correlated with a 3-fold increase in 2-NBDG uptake determined after fixation and subsequent 3D volumetric measurements of the intracellular 2-NBDG content (Figures 5J and 5K), a finding confirmed by determining the ratio of total fluorescence over total protein quantity (Figure 5L). This demonstrated that *Bbs12*$^{-/-}$ adipocytes are the primary site of increased insulin sensitivity and enhanced glucose absorption.

Bbs12-Induced Ciliary Defect Favors MSCs' Adipogenic Program and thereby Contributes to Adipose Tissue Hyperplasia and Increased Cell Autonomous Insulin Sensitivity

To explore the respective roles of hyperphagia and increased calorie load versus enhanced adipogenic differentiation on the development of obesity in BBS, we compared four different groups of male mice, namely WT mice, *Bbs12*$^{-/-}$ mice, hyperphagic *Ob/Ob* mice, and a fourth group of pharmacologically induced adipogenic mice designed as TZD mice. Obesity linked to compulsive feeding behavior in *Ob/Ob* mice has previously been associated with hypertrophic adipose tissue (Calderan et al., 2006). The TZD mice were WT mice with pharmacologically induced adipogenesis by treatment with Troglitazone and Ciglitazone, two thiazolidinedione (TZD) ligands for PPARγ. Examination of visceral adipocytes revealed that *Bbs12*$^{-/-}$ adipocytes were heterogeneous in size with a large proportion of small cells together with larger ones (Figure 6A). On average, these *Bbs12*$^{-/-}$ adipocytes were significantly larger than WT adipocytes (Figure 6B). *Ob/Ob* adipocytes were homogenous and hypertrophic in size compared to WT and *Bbs12*$^{-/-}$ adipocytes whereas TZD-treated adipocytes were heterogeneous in size and significantly smaller than the other groups. Expression

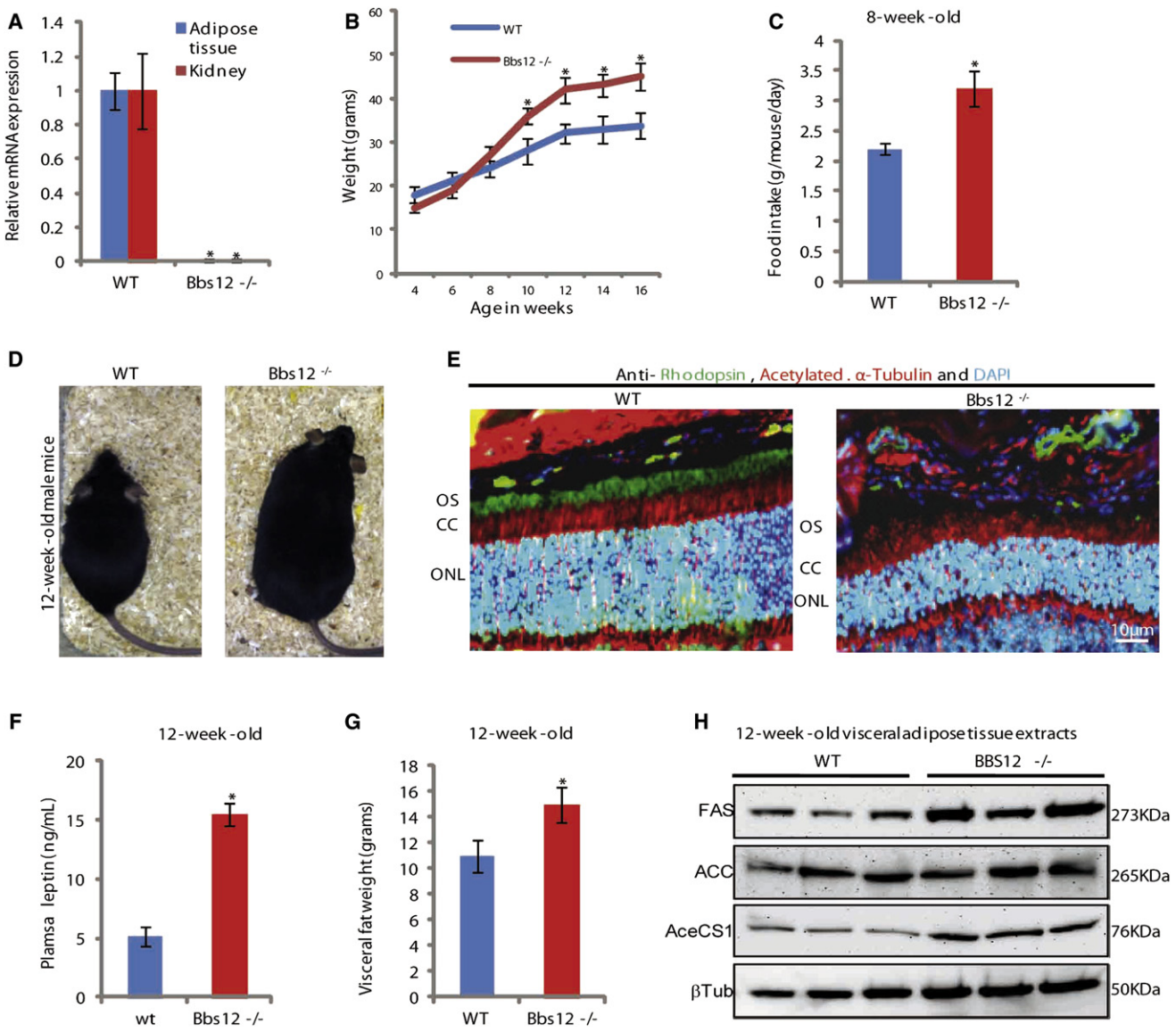

Figure 4. *Bbs12*$^{-/-}$ Male Mouse Phenotype

(A) Relative mRNA expression levels of Bbs12 in target tissues of *Bbs12*$^{-/-}$ and control WT littermates.

(B) Growth curve of *Bbs12*$^{-/-}$ and control WT littermates.

(C) Food intake of 8-week-old *Bbs12*$^{-/-}$ and control WT littermates.

(D) Photograph of *Bbs12*$^{-/-}$ and control WT littermate.

(E) Retinal degeneration in *Bbs12*$^{-/-}$ mouse compared to control WT littermate. OS: outer segment, CC: connecting cilium; ONL: outer nuclear layer (rhodopsin in green, acetylated α-tubulin in red, and nuclei in blue).

(F) Circulating leptin concentrations in *Bbs12*$^{-/-}$ and control WT littermates.

(G) Visceral fat mass of *Bbs12*$^{-/-}$ and control WT littermates.

(H) Adipogenic protein levels in visceral fat.

Values are expressed as mean ± SEM, n = 6–8 in (A), (B), (F), and (G); n = 4 in (C). *p < 0.05 for *Bbs12*$^{-/-}$ versus WT. See also Table S4 and Figure S3.

levels of the sterol regulatory element binding-factor 2 (Srebf2), whose expression directly correlates with adipocyte size (Le Lay et al., 2001), were increased in *Ob/Ob* hypertrophic adipocytes and decreased in both *Bbs12*$^{-/-}$ and TZD adipocytes relative to WT controls (Figure 6C). Interestingly, cell count showed that, on average, there were more cells per unit square are in the *Bbs12*$^{-/-}$ adipose tissue compare to WT ones (Figure 6D).This suggests that hyperplasia plays an important role in adipose tissue expansion in *Bbs12*$^{-/-}$ mice thereby accounting for the greater adiposity of *Bbs12*$^{-/-}$ mice and human BBS patients (Feuillan et al., 2011). IR and GLUT4 protein content in the cellular extracts of adipose tissues from the different mouse groups showed a significant increase of IR and GLUT4 in both *Bbs12*$^{-/-}$ and TZD adipocytes compared to WT

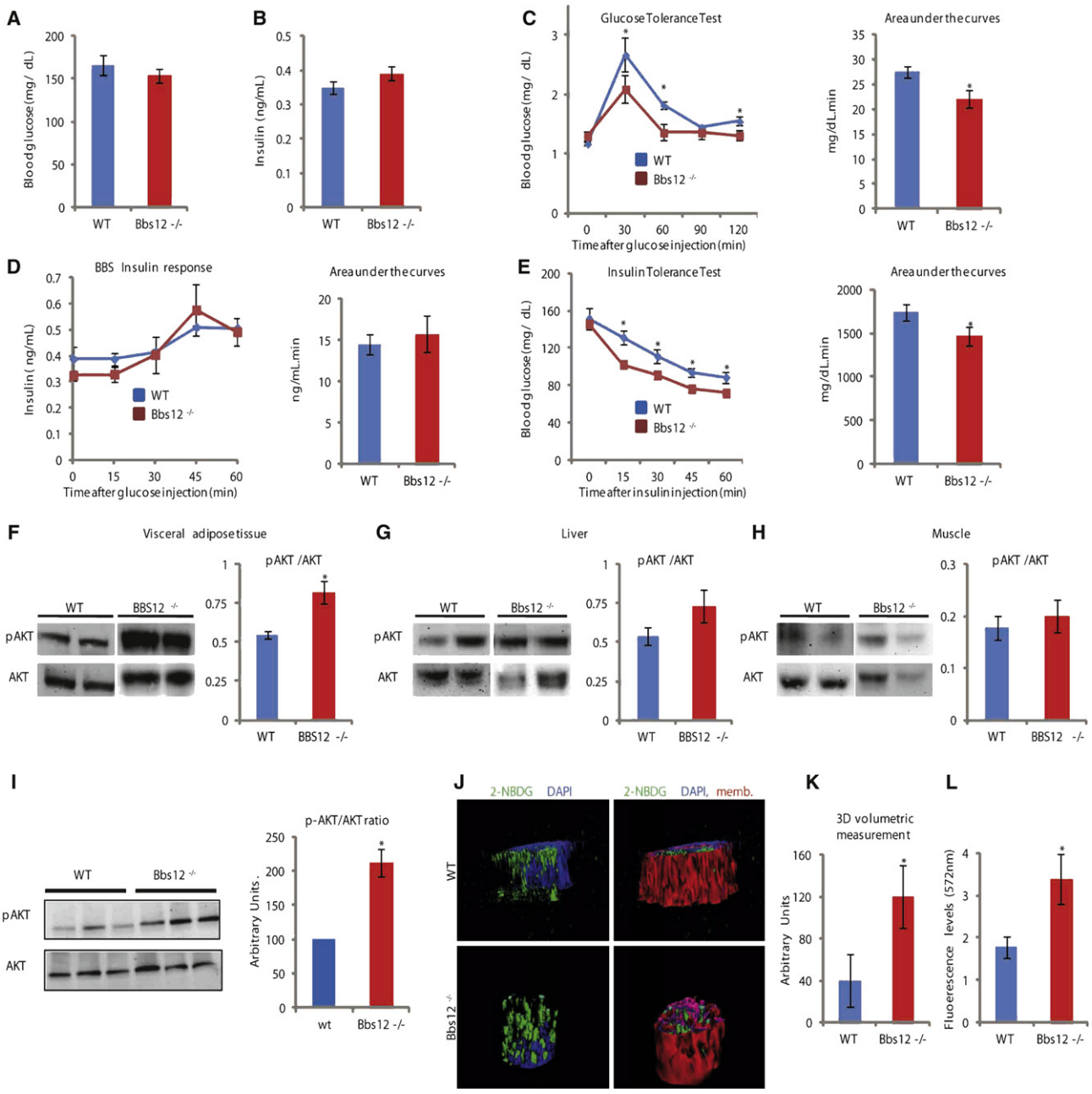

Figure 5. Improved Glucose Metabolism and Insulin Sensitivity of the Adipose Tissue in 12-Week-Old Male *Bbs12*$^{-/-}$ Mice

(A) Fasting blood glucose levels in *Bbs12*$^{-/-}$ and control WT littermates.

(B) Fasting blood insulin levels in *Bbs12*$^{-/-}$ and control WT littermates.

(C) Glucose tolerance tests and corresponding area under the curves.

(D) Insulin response curve and corresponding area under the curves.

(E) Insulin tolerance tests and corresponding area under the curves.

(F) Insulin stimulated phospho-AKT (Ser473) in adipose tissue in *Bbs12*$^{-/-}$ and control WT littermates.

(G) Insulin stimulated phospho-AKT (Ser473) in liver in *Bbs12*$^{-/-}$ and control WT littermates.

(H) Insulin stimulated phospho-AKT (Ser473) in muscle in *Bbs12*$^{-/-}$ and control WT littermates.

(I) Insulin stimulated phospho-AKT (Ser473) in primary adipocytes derived from *Bbs12*$^{-/-}$ and control WT littermates adipose tissues.

(J) 3D image of insulin stimulated 2-NBDG fluorescent glucose analog (green) in primary adipocytes. Plasma membrane in red (Image-iT) and nucleus in blue (DAPI).

(K) 3D volumetric determination of intracellular 2-NBDG content in primary adipocytes.

(L) Ratio of fluorescent levels of intracellular 2-NBDG content/total protein quantity.

Values are expressed as mean ± SEM; n = 6–8 in (A), (B), (C), (D), and (E). n = 60 per mouse with 3 mice per genotype in K. n = 6 wells per condition in L *$p < 0.05$ for *Bbs12*$^{-/-}$ versus WT. All mice were fed ad libitum on defined 45% fat chow. See also Figure S4.

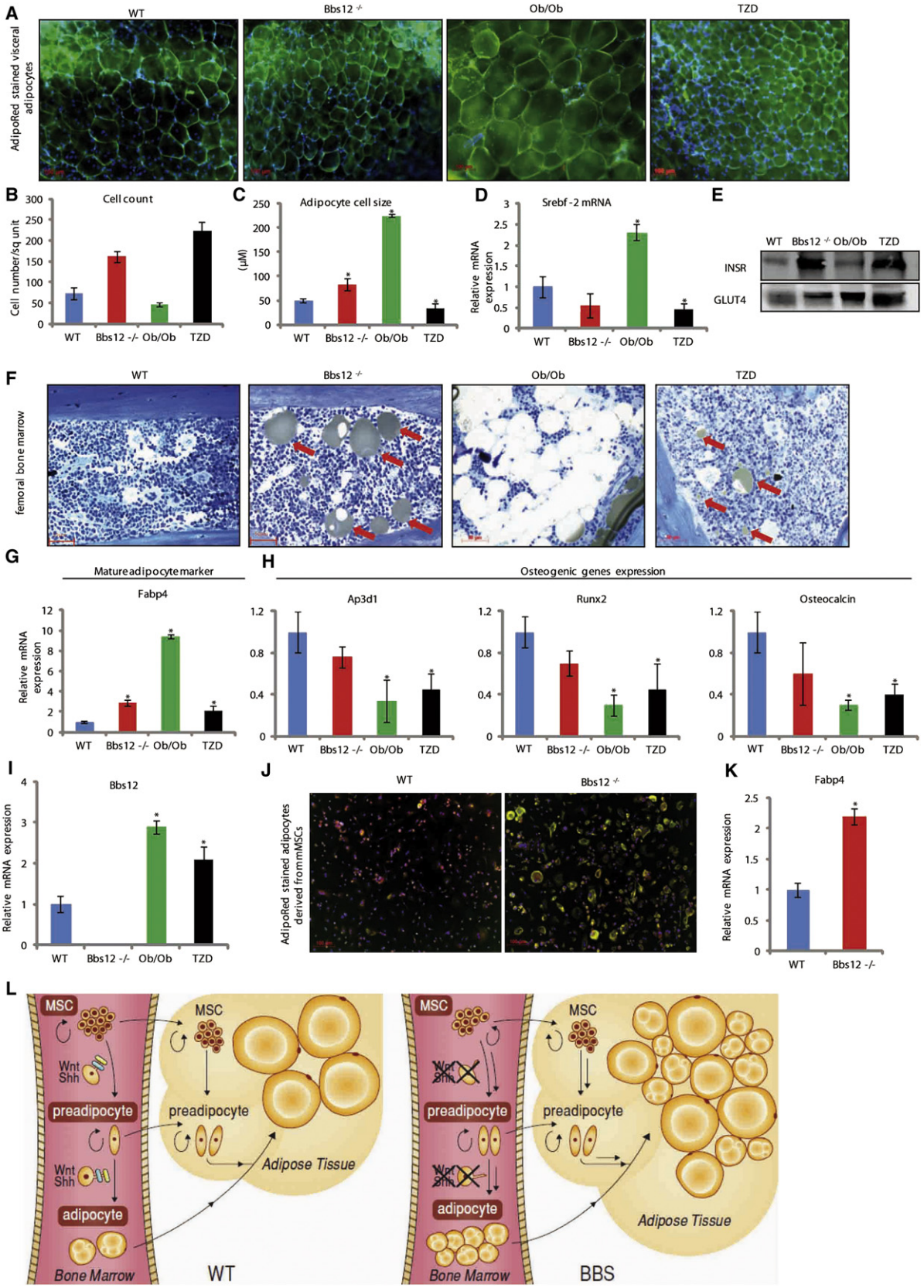
A
WT
Bbs12 -/-
Ob/Ob
TZD
AdipoRed stained visceral adipocytes
B
Cell count
Cell number/sq unit
WT Bbs12 -/- Ob/Ob TZD
C
Adipocyte cell size
(μM)
D
Srebf -2 mRNA
Relative mRNA expression
E
INSR
GLUT4
F
femoral bone marrow
G
Mature adipocyte marker
Fabp4
H
Osteogenic genes expression
Ap3d1
Runx2
Osteocalcin
I
Bbs12
J
AdipoRed stained adipocytes derived from MSCs
K
Fabp4
L
MSC
Wnt
Shh
preadipocyte
adipocyte
Adipose Tissue
Bone Marrow
WT
BBS

controls (Figures 6E and S5), corroborating the initial in vitro results described in Figure 3A.

To clarify the basis of the heterogeneity of cell size of adipocytes in the *Bbs12*$^{-/-}$ mice, we compared the femoral bone marrows (BM) from the four different mouse groups (Figure 6F). A small number of mature adipocytes (arrows; Figure 6F) were found inside the BM of *Bbs12*$^{-/-}$ and TZD mice but none in the WT. On the other hand, the BM of the *Ob*/*Ob* was almost completely replaced with mature adipocytes. These findings were confirmed by the finding of increased expression levels of adipocyte fatty acid-binding protein (Fabp4) (Figure 6G), a marker for mature adipocytes (Balzar et al., 2011), in the BM of *Ob*/*Ob, Bbs12*$^{-/-}$, and TZD mice compared to WT. Owing to the crosstalk taking place in MSCs between adipogenic and osteoblastic differentiation (Muruganandan et al., 2009), any condition that activates adipogenesis such as the *Bbs12*$^{-/-}$, *Ob*/Ob, and the TZD (Gimble et al., 1996) phenotypes, inevitably impacts the osteoblastic differentiation process. We therefore determined the expression levels of three osteoblastic genes (*Ap3d1*, *Runx2*, and *Osteocalcin*) and found a reduction of all three genes in the BM of *Ob*/*Ob, Bbs12*$^{-/-}$, and TZD mice compared to WT, albeit nonsignificant in the *Bbs12*$^{-/-}$ group (Figure 6H).

Remarkably, in the TZD and the *Ob*/*Ob* BM, Bbs12 expression levels were significantly increased (Figure 6I), validating previous in vitro results (Marion et al., 2009) that during adipogenic differentiation, Bbs12 expression is increased. We also wanted to know whether the enhanced adipogenic program exhibited by the MSCs was intrinsically related to the in-cell BBS12-induced defect or whether there could be another factor favoring the differentiation. To address this question, mouse MSCs (mMSCs) from WT and *Bbs12*$^{-/-}$ mice were isolated, cultured, and characterized (Figure S6), before adipogenesis was triggered (Figure 6J). *Bbs12*$^{-/-}$ mMSCs reproduced the same phenotype as the Bbs12-RNAi treated hMSCs; namely, they demonstrated an enhanced adipogenic program leading to higher intracellular triglyceride contents and increased *Fabp4* expression (Figure 6K), consistent with enhanced BBS12 expression during adipogenesis acting as an adipogenic brake, which is released when BBS is absent or inhibited.

A model encompassing the effect of the BBS-induced impact on adipogenic differentiation is depicted in Figure 6L. In the WT condition, MSC differentiation toward adipocytes is tightly regulated by the Wnt and Shh antiadipogenic signaling pathways in which the primary cilium plays a key functional role (Fontaine et al., 2008; Suh et al., 2006). The equilibrium between pro- and antiadipogenic signals results in MSC differentiation into homogenously sized adipocytes in WT animals. Conversely, primary cilium dysfunction through BBS12 inactivation disables these antiadipogenic brakes, thereby facilitating the recruitment of MSCs toward adipogenic differentiation. The end result of this enhanced recruitment of MSCs into adipocytes in BBS is an increased, heterogeneously sized population of adipocytes with high IR and GLUT4 expression—a consistent finding reproduced in human patients with BBS, human, and mouse MSC cultures and *Bbs12*$^{-/-}$ mice as seen in this study.

Adipocyte Function in *Bbs12*$^{-/-}$ Mice and Inflammation

The rate of free fatty acid (FFA) mobilization from the adipose tissue to the portal vein correlates with insulin resistance and is associated with inflammatory response in macrophages. Circulating FFA was lower in *Bbs12*$^{-/-}$ (Figure 7A), and upon insulin injection, FFA suppression was significantly higher in the *Bbs12*$^{-/-}$ (Figure 7B). These results confirmed a higher adipose tissue insulin sensitivity of the *Bbs12*$^{-/-}$ adipose tissue. Adipokine measurements showed increased levels of Adiponectin (Figure 7C) and decreased levels of Resistin (Figure 7D), highlighting an adipokine profile favoring insulin sensitivity in the *Bbs12*$^{-/-}$ mice. Inflammation is a major cause of insulin resistance in the adipose tissue associated with accumulation of activated macrophages in the adipose tissue, and their quantities correlate with measures of insulin resistance (Greenberg and Obin, 2006; Shoelson et al., 2006b). Recruitment and proinflammatory activation of adipose tissue macrophages are required for the development of diabetes with obesity. Recruitment is mainly governed by the level of the monocyte chemoattractant protein-1 (MCP-1) (Kanda et al., 2006), and circulating MCP-1 levels were similar in *Bbs12*$^{-/-}$ and WT controls when normalized with body weight (Figure 7E). Macrophages are plastic cells with two distinct flavors (Gordon and Taylor, 2005; Mantovani et al., 2004), either the proinflammatory M1 flavor secreting high levels of proinflammatory mediators such as TNFα and IL-6 (Harkins et al., 2004; Xu et al., 2003) or the M2 flavor. The later represent a group of macrophages with low proinflammatory cytokine producers and instead generate high levels of antiinflammatory cytokines like IL10 (Gordon, 2003). Interestingly, circulating IL-6 levels were not different between the tested groups whereas TNFα levels were significantly lower

Figure 6. Bbs12 Inactivation Favors Adipogenesis in the Bone Marrow Causing Adipose Tissue Hyperplasia

(A) AdipoRed stained adipocytes from 40 g male mice with corresponding genotype and treatment.
(B) Adipocyte cell count from 40 g male mice with corresponding genotype and treatment.
(C) Adipocyte cell size measurements from 40 g male mice with corresponding genotype and treatment.
(D) Relative mRNA expression levels of Srebf2 in corresponding adipose tissue.
(E) IR and GLUT4 protein levels in corresponding visceral adipose tissues.
(F) Toluidin blue staining of femoral BM (arrows indicate adipocytes).
(G) Relative mRNA expression levels of Fabp4 in corresponding BM extracts.
(H) Relative mRNA expression levels of osteogenic genes in corresponding BM extracts.
(I) Relative mRNA expression of *Bbs12* in the BM.
(J) AdipoRed-stained adipocytes derived ex vivo from primary mouse MSCs (mMSCs).
(K) Relative mRNA expression levels of *Fabp4* in adipocytes derived mMSCs.
(L) Schematic representation of the BBS impact on MSC recruitment from the bone marrow to the adipose tissue.
Values are expressed as mean ± SEM. In (B) and (C), n = 200 per mouse with 3 mice per group. n = 4 in (G), (H), (I), and (K). *p < 0.05 for tested group versus WT.
*p < 0.05 for tested group versus WT. See also Figures S5 and S6.

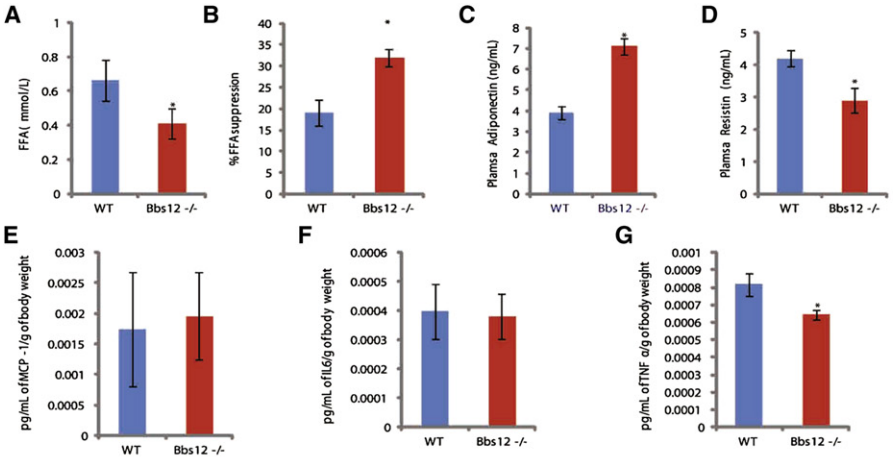

H

Gene Name	Function	Fold change	Resampling p-value
eNOS	Vascularisation marker	1,842093622	0,0156
Adiponectin	anti-diabetic &anti-inflammatory adipokine	2,177078035	0,0212
Il13	Cytokine.Inhibits inflammatory cytokine production	1,97166333	0,02716
Il10	Cytokine improving insulin resistance (anti-diabetic)	1,926307211	0,01982
Arg1	Marker of M2 flavored macrophages (tolerance)	2,45882725	0,00176
Cd68	macrophage marker	-2,046257914	0,0304
Mcp-1	chemotactic agent attracting monocytes (pro-inflammatory)	-2,056108422	0,00613
iNOS	marker of M1 flavored macrophages (pro-inflammatory)	-1,30007017	0,02006
Tnf α	Pro-inflammatory cytokine	-1,8899926	0,00866
Cox1	Constitutive pro-inflammatory enzyme	-1,7933208	0,00478
Serpine1 (PAI1)	Plasminogen activator inhibitor-1 controls fibrinolysis	-1,93516781	0,0182
Resistin	Adipokine suppressing insulin-mediated glucose uptake in adipocytes (pro-diabetic)	-2,53573472	0,0306
Il4	Cytokine inducing aTh2 response (tolerance)	1,529377915	0,776
Cox2	Inducible pro-inflammatory enzyme	1,014819018	0,6334
Ifn γ	pro-inflammatory cytokine	-1,61830121	0,2882
Il2	chemotractant forwhite blood cells	1,082660414	0,1474
Il4	induces the expression of class II MHC molecules on resting B-cells	1,061149076	0,973
Arg2	Marker of M2 flavored macrophages (tolerance)	1,033478452	0,9698
Il1b	Cytokine produced by activated macrophages and mediates inflammatory response	1,094955484	0,486
Icam1	adhesion molecule involved in leukocyte trans-endothelial migration	1,044133584	0,6752
Vcam1	adhesion molecule involved in leukocyte emigration to sites of inflammation	-1,55248579	0,0306
Fibrinogen	inflammatory marker in adipose tissue	1,125030283	0,961
Vwf	inflammatory marker in adipose tissue	1,170670465	0,2912
Ucp1	Brown fat marker	-1,000115233	0,6677

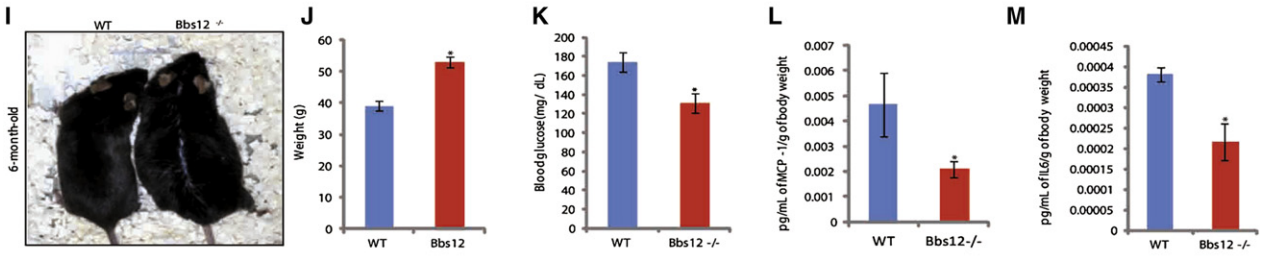

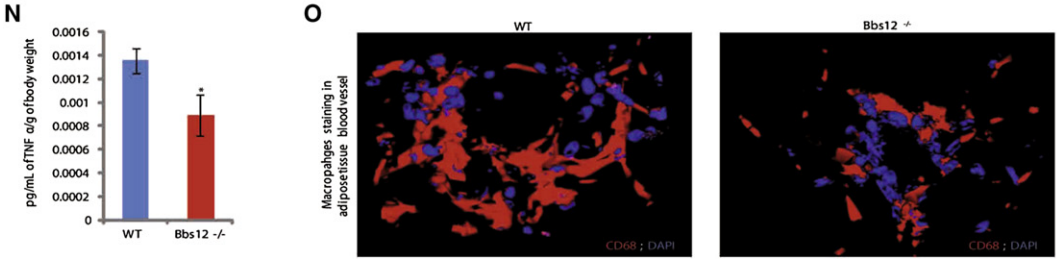

in the *Bbs12*$^{-/-}$ mice. These findings show that the *Bbs12*$^{-/-}$ mice are systemically not inflamed.

We next investigated the inflammatory gene-expression profile in the adipose tissue. For that, we compared gene-expression profile in peri-renal white adipose tissue from 40 g male *Bbs12*$^{-/-}$ mice and WT age-controls mice (Figure 7H). Interestingly, a selection of anti-inflammatory genes (*eNOS*, *Adiponectin*, *IL13* [Gordon, 2003], *IL10*, *and Arginase1* [*Arg1*] [Bronte and Zanovello, 2005]) were significantly upregulated. Alternatively, select proinflammatory genes (*Cd68*, *Mcp-1*, *iNos*, *Tnfα*, *Cox1*, *Serpine*, and *Resistin*) were significantly downregulated, while other immunorelated genes were similar. In aggregate, these findings highlight the absence of low-grade inflammation in the obese *Bbs12*$^{-/-}$ adipose tissue.

The observed protective phenotype of BBS was next tested in diet-induced obesity challenged mice. Male *Bbs12*$^{-/-}$ mice at 6-month-old became massively obese (on average 54 g), whereas the WT controls remained at 40 g (Figure 7I and 7J). Blood glucose levels in overnight fasted animals were significantly higher in WT mice compared to the *Bbs12*$^{-/-}$ (Figure 7K). Concurrently, all measured proinflammatory markers (MCP-1, IL-6, and TNF-α) were higher in the WT group compared to the *Bbs12*$^{-/-}$ (Figures 7L–7N). Concomitant with the proinflammatory cytokine profile, there was a significant increase in macrophage infiltration in the adipose tissue of the WT compared to the *Bbs12*$^{-/-}$ (Figure 7O). These results demonstrate that the primary cilium regulates the maturation and function of the adipose tissue. Moreover, a disruption in this ciliary control is able to favor adiposity while preventing deleterious inflammatory response.

DISCUSSION

Obesity is a cardinal clinical feature of BBS, and yet, unlike other obesity associated ciliopathies such as Alstrom Syndrome, based on our observations and those of others (Feuillan et al., 2011), surprisingly T2DM is not per se a common feature of BBS. Indeed we show here that *Bbs12*$^{-/-}$ mice despite obesity have significantly greater glucose tolerance and insulin sensitivity than lean WT control littermates. Examination of the effects of inactivation of the ciliary protein BBS12 in human bone marrow MSC showed that absence of BBS12 favored programming of MSC toward adipocyte differentiation through simultaneous inhibition of antiadipogenic, and activation of proadipogenic, pathways. This results in increased glucose uptake and triglyceride synthesis capacity together with low levels of local inflammatory response in the adipose tissue.

Although not a defining trait of the BBS, diabetes has historically been considered as a secondary feature of this ciliopathy. It is indeed true that throughout literature, it has been described that a minority of BBS patients developed type 2 diabetes (Webb et al., 2009), including our own previous published data (Imhoff et al., 2011). It is therefore surprising that BBS inactivation can actually be protective against diabetes. Several reasons can explain this apparent discrepancy observed in the human conditions. One reason is that, historically BBS like the other related ciliopathies was diagnosed based on the association of characteristic clinical features. But with the advent of high-throughput sequencing and the discovery of the continuously increasing number of identified of genes involved in these ciliopathies (with the new BBS17 recently identified in our lab [Marion et al., 2012]), we are now more able to make clearer distinctions between the BBS and the other related ciliopathies. For instance, we were recently able to illustrate the pitfall of purely based clinical categorization of the BBS where patients who were clinically suspected of having BBS were actually mutated in the Alms1 gene, the other ciliopathy mainly characterized by obesity and diabetes (Aliferis et al., 2012). Second, a so far underestimated reason that explains that a minority of BBS patients may develop diabetes is what is nowadays considered as phenotypic variation. As described in a *Scientific Perspective* entitled *Mendelian Puzzles* (Chakravarti and Kapoor, 2012), not all individuals with an identical mutation are equally affected. Indeed, the idea that a single mutation in one gene causes the clinical phenotype is evolving as human genetics keep evolving from a focus of single genes into a more genomic view. This means that all sorts of interacting genetic variants may give rise to different degree of dysfunction. This applied to the BBS might explain the diabetes phenotype in this minority of BBS patients, a feature that warrants more research.

Interestingly, the fact that chaperone BBS proteins are only maximally expressed during MSC differentiation suggests that

Figure 7. Decreased Adipose Tissue Inflammation in *Bbs12*$^{-/-}$ Mice

(A) Blood FFA levels in 12-week-old mice.
(B) Insulin-stimulated percentage of FFA suppression in 12-week-old mice.
(C) Circulating Adiponectin in WT and *Bbs12*$^{-/-}$ mice in 12-week-old mice.
(D) Circulating Resistin in WT and *Bbs12*$^{-/-}$ mice in 12-week-old mice.
(E) Circulating TNF-α correlated to body weight in 12-week-old mice.
(F) Circulating IL-6 correlated to body weight in 12-week-old mice.
(G) Circulating MCP-1 correlated to body weight in 12-week-old mice.
(H) Table showing a group of selected genes, function, fold change in *Bbs12*$^{-/-}$ adipose tissue compared to WT. In green: genes expression increased; in red: gene expression decreased; in black: gene expression similar.
(I) Photograph of 6-month-old mice fed with 45% fat and 35%carbohydrate.
(J) Body weight of male mice weight at 6 months.
(K) Blood glucose level in 6-month-old mice.
(L) Circulating MCP-1 correlated to body weight in 6-month-old mice.
(M) Circulating IL-6 correlated to body weight in 6-month-old mice.
(N) Circulating TNF-α correlated to body weight in 6-month-old mice.
(O) 3D images of adipose tissue blood vessels immunostained for macrophages (CD68 in red) and nuclei (DAPI).
Values are expressed as mean ± SEM; n = 6–8 in (A)–(G) and in (J)–(N); n = 4 in (H). *$p < 0.05$ for tested group versus WT.

their main action may be restricted to primary cilium biogenesis and BBS proteins may not be involved in mature adipocyte function. This is supported by the fact that inactivation of BBS proteins in mature adipocytes resulted in no detectable effects (Figure S7). Most of the BBS proteins share the same expression profile (Forti et al., 2007; Marion et al., 2009) and form an interaction complex (Jin et al., 2010; Nachury et al., 2007), suggesting they should have a common role in MSC differentiation. BBS proteins are not the only ciliary proteins impacting on adipogenesis if inactivated. Partial in vivo inactivation of Polycystin 1 (*Pkd1*), another ciliary protein, activated adipogenesis in mouse bone marrow (Qiu et al., 2010). Surprisingly, this proadipogenic effect of *Pkd1* inactivation was reversed by concomitant partial decrease of another ciliary protein, *Kif3a*. These data provide evidence of the coexistence of two distinct groups of ciliary proteins, one whose action is antiadipogenic such that their inactivation is proadipogenic, like *Bbs12* and *Pkd1*, and one whose action is proadipogenic such that their inactivation is antiadipogenic, like *Kif3a*. These findings indicate that ciliary proteins likely act as gatekeepers, controlling the progression of cells through adipocyte differentiation. This process of controlling adipocyte recruitment towards the adipose tissue is most probably the origin of the lack of inflammatory response observed in the *Bbs12*$^{-/-}$ mice and most probably in the patients, too. Inflammatory response is triggered by a poor access of oxygen and food supply to the mature adipocytes in overdeveloped tissue. This eventually leads to cellular death thereby activating the inflammatory cascade. Inactivation of BBS proteins activates the recruitment of precursor cells to the adipose tissue, thereby creating a continuous refurnishing of small adipocytes in the adipose tissue. These new cells prevent the already existing mature adipocytes to absorb excessive glucose to become hypertrophic and thereby prevent low-grade inflammation, the condition responsible for insulin resistance of the adipose tissue.

Remarkably, preadipocytes derived from patients with T2DM have been described as less prone to adipogenic differentiation (van Tienen et al., 2011), suggesting that resistance of preadipocytes to adipogenic differentiation may be an important contributor to insulin resistance. The opposite effect is observed in patients with BBS who have increased adipogenic differentiation with consequent enhanced insulin sensitivity and increased adipocyte glucose uptake capacity. This explains why even morbidly obese BBS patients have a disproportionately low frequency and severity of T2DM. Although the adipose tissue is clearly more insulin sensitive and has a higher glucose absorptive capacity, we cannot totally exclude some other parameters contributing to the overall phenotype. A hallmark of T2DM is adipose tissue insulin resistance, with this being the target of the TZD family of antidiabetic drugs that act to lower plasma glucose levels at least in part by increasing the number of small-sized adipocytes (MacKellar et al., 2009). The phenotype resulting from the BBS-associated ciliary defect in adipose tissue mimics the effect of TZD, namely adipose tissue hyperplasia associated with increased insulin sensitivity.

Our data shows that *Bbs12*$^{-/-}$ adipose tissue is heterogeneous with a mixture of both hyperplasia and hypertrophy, suggesting the obesity in BBS is due to a combination of hypothalamic hyperphagia plus increased recruitment of adipocyte progenitors. High plasma leptin levels in BBS patients (and *Bbs12*$^{-/-}$ mice) does not correlate with patient adiposity (Feuillan et al., 2011), suggesting intrinsic leptin resistance in BBS. This likely reflects the failure of the leptin receptor to be targeted to the primary cilium resulting in incapacity of leptin-responsive neurons to respond to leptin (Seo et al., 2009). This implies that in BBS, the downstream targets of the Leptin receptor fail to be activated, including Signal transducer and activator of transcription (Stat)-3 and Phosphoinositide 3-kinase (PI3K) signaling in POMC neurons. In support, impairment of central leptin-mediated PI3K signaling induced hepatic steatosis and excessive TG accumulation in the liver that was independent of hyperphagia and obesity (Warne et al., 2011). In addition, adipose tissue dysfunction has been linked to nonalcoholic hepatic steatosis (Duval et al., 2010). To identify if the BBS phenotype was prosteatotic, we determined the hepatic TG content and found a 3-fold increase in the *Bbs12*$^{-/-}$ compared to a 14-fold increase in *Ob*/*Ob* mice and no change in TZD mice (Figures S7C and S7D). The fact that BBS livers were less steatotic compared to *Ob*/*Ob* livers suggests partial residual leptin signaling in the hypothalamus—a finding previously described in *Bbs2, 4,* and *6* knockout mice where Pomc expression levels were, although decreased, still expressed (Rahmouni et al., 2008b).

While these observations might nevertheless suggest a decrease in leptin in BBS by way of feedback, extremely high leptinaemia was observed in both humans and mice with BBS. This could be explained by the fact that adipocytes secrete leptin in response to insulin and, most importantly, proportionately to the amount of glucose absorbed (Mueller et al., 1998). With maintained insulin levels and increased glucose absorption capacity, we showed that BBS adipocytes in vitro secreted more leptin, a finding previously observed in adipocytes derived from dermal fibroblasts of our patients with BBS (Marion et al., 2009). The fact that leptin secretion was reduced in the presence of cytochalasin B, an inhibitor of glucose absorption (Figure S7E), confirms the direct link between increased glucose absorption and increased adipocyte leptin secretion in BBS. In aggregate, this suggests that the BBS phenotype is a combination of adipocyte-mediated hyperleptinaemia with partial leptin resistance in the hypothalamus.

An intriguing finding was the normal fasting plasma insulin levels in the *Bbs12*$^{-/-}$ mice despite the increased in vivo, ex vivo, and in vitro insulin sensitivity of BBS12-deficient adipocytes. The expected effect of increased cell autonomous insulin sensitivity would be a reduction in fasting insulin levels. As increased pancreatic islet size was reported as a key feature of obese diabetic models such as *Ob*/*Ob* (Yokoi, 2010) or Alstrom's Foz/foz mice (Arsov et al., 2006), we examined the pancreas of *Bbs12*$^{-/-}$ mice but found no increase in islet size (mean surface area ~70000 μm^2; data not shown). These findings seem to indicate that the insulin level might be influenced by another tissue that is also impacted in the BBS—an area that warrants further investigations. Also, insulin regulates glucose homeostasis primarily through suppression of hepatic glucose production and stimulation of peripheral glucose uptake, primarily in the muscle and to a lesser extent in the adipose tissue (DeFronzo et al., 1985; Weyer et al., 1999). Therefore, even in obesity, the contribution of the adipose tissue to glucose uptake

compared to liver or muscle uptake remained rather low. In the BBS condition, even though the adipose tissue is bigger and more sensitive to insulin and has a higher capacity for glucose absorption, it cannot by itself regulate the overall glucose homeostasis. A probable parameter of the adipose tissue impacting systemic glucose levels in the BBS patients and the BBS models could be the low level of low-grade inflammation of the adipose tissue. How and to what extent the absence of inflammatory stimuli in the BBS contributes in preventing insulin resistance will require further investigations.

In conclusion, although human ciliopathies are extremely rare conditions, they provide opportunity for unique insights into key cellular pathways including those involved in adipocyte differentiation, obesity, and insulin resistance. In particular, the disconnect between obesity and T2DM in BBS suggests that modulation of primary cilia regulation of adipogenic pathways, most probably by regulating the enzymatic activity of some BBS proteins such as BBS3, may be a potential target for reversal of obesity-associated insulin resistance and T2DM.

EXPERIMENTAL PROCEDURES

Human Tests and Samples

The subcutaneous adipose tissue biopsies, glucose tolerance tests, and insulin response curves were performed on BBS patients (see Farha et al. [2011] and Marion et al. [2011] for age, sex, pedigree, and phenotype) studied as part of a clinical research protocol in the *Protocole Hospitalier de Recherche Clinique National Program* (*PHRC*) undertaken at the University Hospital of Strasbourg, France. No studied patient had renal dialysis or renal transplantation. Patients provided written informed consent under the authority of the local ethics committee. The adipose tissue sample at a depth of 1 cm beneath the skin was obtained after a biopsy procedure (available on request) performed by a plastic surgeon on the abdominal fat tissue.

Animal Treatment

They were individually caged and fed ad libitum. The defined 45% fat chow (Research Diets D06011802) was used also to feed the KO mice and WT controls as the Ob/Ob mice were fed with this diet at Jackson Labs until they reached the 40 g threshold. They were then euthanized by decapitation for analysis. For the TZD treatment, a combination of both ciglitizone and troglitazone at a concentration of 250 μg/kg body weight/day each (to prevent steatotic side effects in the hepatocytes) was added to the drinking water and was given to the mice sharing the same genetic mixed background as the *Bbs12*$^{-/-}$. These mice were fed on the same commercial high fat diet ad libitum for a 1 month period initiated at 12 weeks postnatal. To challenge the mice for obesity and diabetes, we fed a group of male mice with a diabetic inducing diet (45 kcal% fat and 35 kcal% carbohydrate) (Research Diets D12451) for 6 months and then carried the analysis.

SUPPLEMENTAL INFORMATION

Supplemental Information includes seven figures, five tables, Supplemental Experimental Procedures, and Supplemental References and can be found with this article online at http://dx.doi.org/10.1016/j.cmet.2012.08.005.

ACKNOWLEDGMENTS

We thank RETINA France, UNADEV and all the patients' associations. We thank D. DEMBELE for the Agilent data analysis, J-M Egly and W. Lamers for their critical reading of the manuscript and the Mouse Clinic Institute for generating the Bbs12 knockout mice. This study was supported by grants from the ANR Call for Rare Disease 2006 and 2009), the INSERM Avenir Program and by the PHRC 2007.

Received: February 28, 2012
Revised: June 13, 2012
Accepted: August 16, 2012
Published online: September 4, 2012

REFERENCES

Aliferis, K., Hellé, S., Gyapay, G., Duchatelet, S., Stoetzel, C., Mandel, J.L., and Dollfus, H. (2012). Differentiating Alström from Bardet-Biedl syndrome (BBS) using systematic ciliopathy genes sequencing. Ophthalmic Genet. *33*, 18–22.

Arsov, T., Silva, D.G., O'Bryan, M.K., Sainsbury, A., Lee, N.J., Kennedy, C., Manji, S.S., Nelms, K., Liu, C., Vinuesa, C.G., et al. (2006). Fat aussie—a new Alström syndrome mouse showing a critical role for ALMS1 in obesity, diabetes, and spermatogenesis. Mol. Endocrinol. *20*, 1610–1622.

Balzar, S., Fajt, M.L., Comhair, S.A., Erzurum, S.C., Bleecker, E., Busse, W.W., Castro, M., Gaston, B., Israel, E., Schwartz, L.B., et al. (2011). Mast cell phenotype, location, and activation in severe asthma. Data from the Severe Asthma Research Program. Am. J. Respir. Crit. Care Med. *183*, 299–309.

Batchvarova, N., Wang, X.Z., and Ron, D. (1995). Inhibition of adipogenesis by the stress-induced protein CHOP (Gadd153). EMBO J. *14*, 4654–4661.

Beales, P.L. (2005). Lifting the lid on Pandora's box: the Bardet-Biedl syndrome. Curr. Opin. Genet. Dev. *15*, 315–323.

Berbari, N.F., Lewis, J.S., Bishop, G.A., Askwith, C.C., and Mykytyn, K. (2008). Bardet-Biedl syndrome proteins are required for the localization of G protein-coupled receptors to primary cilia. Proc. Natl. Acad. Sci. USA *105*, 4242–4246.

Berger, J., Bailey, P., Biswas, C., Cullinan, C.A., Doebber, T.W., Hayes, N.S., Saperstein, R., Smith, R.G., and Leibowitz, M.D. (1996). Thiazolidinediones produce a conformational change in peroxisomal proliferator-activated receptor-gamma: binding and activation correlate with antidiabetic actions in db/db mice. Endocrinology *137*, 4189–4195.

Bronte, V., and Zanovello, P. (2005). Regulation of immune responses by L-arginine metabolism. Nat. Rev. Immunol. *5*, 641–654.

Calderan, L., Marzola, P., Nicolato, E., Fabene, P.F., Milanese, C., Bernardi, P., Giordano, A., Cinti, S., and Sbarbati, A. (2006). In vivo phenotyping of the ob/ob mouse by magnetic resonance imaging and 1H-magnetic resonance spectroscopy. Obesity (Silver Spring) *14*, 405–414.

Cardenas-Rodriguez, M., and Badano, J.L. (2009). Ciliary biology: understanding the cellular and genetic basis of human ciliopathies. Am. J. Med. Genet. C. Semin. Med. Genet. *151C*, 263–280.

Chakravarti, A., and Kapoor, A. (2012). Genetics. Mendelian puzzles. Science *335*, 930–931.

Chiarelli, F., and Di Marzio, D. (2008). Peroxisome proliferator-activated receptor-gamma agonists and diabetes: current evidence and future perspectives. Vasc. Health Risk Manag. *4*, 297–304.

Choi, S.S., Cha, B.Y., Iida, K., Lee, Y.S., Yonezawa, T., Teruya, T., Nagai, K., and Woo, J.T. (2011). Artepillin C, as a PPARγ ligand, enhances adipocyte differentiation and glucose uptake in 3T3-L1 cells. Biochem. Pharmacol. *81*, 925–933.

Cristancho, A.G., and Lazar, M.A. (2011). Forming functional fat: a growing understanding of adipocyte differentiation. Nat. Rev. Mol. Cell Biol. *12*, 722–734.

de Foresta, B., Vincent, M., Garrigos, M., and Gallay, J. (2011). Transverse and tangential orientation of predicted transmembrane fragments 4 and 10 from the human multidrug resistance protein (hMRP1/ABCC1) in membrane mimics. Eur. Biophys. J. *40*, 1043–1060.

DeFronzo, R.A., Gunnarsson, R., Björkman, O., Olsson, M., and Wahren, J. (1985). Effects of insulin on peripheral and splanchnic glucose metabolism in noninsulin-dependent (type II) diabetes mellitus. J. Clin. Invest. *76*, 149–155.

Duval, C., Thissen, U., Keshtkar, S., Accart, B., Stienstra, R., Boekschoten, M.V., Roskams, T., Kersten, S., and Müller, M. (2010). Adipose tissue dysfunction signals progression of hepatic steatosis towards nonalcoholic steatohepatitis in C57BL/6 mice. Diabetes *59*, 3181–3191.

Farha, S., Asosingh, K., Xu, W., Sharp, J., George, D., Comhair, S., Park, M., Tang, W.H., Loyd, J.E., Theil, K., et al. (2011). Hypoxia-inducible factors in

human pulmonary arterial hypertension: a link to the intrinsic myeloid abnormalities. Blood *117*, 3485–3493.

Feuillan, P.P., Ng, D., Han, J.C., Sapp, J.C., Wetsch, K., Spaulding, E., Zheng, Y.C., Caruso, R.C., Brooks, B.P., Johnston, J.J., et al. (2011). Patients with Bardet-Biedl syndrome have hyperleptinemia suggestive of leptin resistance. J. Clin. Endocrinol. Metab. *96*, E528–E535.

Fontaine, C., Cousin, W., Plaisant, M., Dani, C., and Peraldi, P. (2008). Hedgehog signaling alters adipocyte maturation of human mesenchymal stem cells. Stem Cells *26*, 1037–1046.

Forti, E., Aksanov, O., and Birk, R.Z. (2007). Temporal expression pattern of Bardet-Biedl syndrome genes in adipogenesis. Int. J. Biochem. Cell Biol. *39*, 1055–1062.

Généreux, P., Mehran, R., Palmerini, T., Caixeta, A., Kirtane, A.J., Lansky, A.J., Brodie, B.R., Witzenbichler, B., Mockel, M., Guagliumi, G., et al; HORIZONS-AMI Trial Investigators. (2011). Radial access in patients with ST-segment elevation myocardial infarction undergoing primary angioplasty in acute myocardial infarction: the HORIZONS-AMI trial. EuroIntervention *7*, 905–916.

Gimble, J.M., Robinson, C.E., Wu, X., Kelly, K.A., Rodriguez, B.R., Kliewer, S.A., Lehmann, J.M., and Morris, D.C. (1996). Peroxisome proliferator-activated receptor-gamma activation by thiazolidinediones induces adipogenesis in bone marrow stromal cells. Mol. Pharmacol. *50*, 1087–1094.

Girard, D., and Petrovsky, N. (2011). Alström syndrome: insights into the pathogenesis of metabolic disorders. Nat. Rev. Endocrinol. *7*, 77–88.

Gordon, S. (2003). Alternative activation of macrophages. Nat. Rev. Immunol. *3*, 23–35.

Gordon, S., and Taylor, P.R. (2005). Monocyte and macrophage heterogeneity. Nat. Rev. Immunol. *5*, 953–964.

Greenberg, A.S., and Obin, M.S. (2006). Obesity and the role of adipose tissue in inflammation and metabolism. Am. J. Clin. Nutr. *83*, 461S–465S.

Harkins, J.M., Moustaid-Moussa, N., Chung, Y.J., Penner, K.M., Pestka, J.J., North, C.M., and Claycombe, K.J. (2004). Expression of interleukin-6 is greater in preadipocytes than in adipocytes of 3T3-L1 cells and C57BL/6J and ob/ob mice. J. Nutr. *134*, 2673–2677.

Hildebrandt, F., Benzing, T., and Katsanis, N. (2011). Ciliopathies. N. Engl. J. Med. *364*, 1533–1543.

Imhoff, O., Marion, V., Stoetzel, C., Durand, M., Holder, M., Sigaudy, S., Sarda, P., Hamel, C.P., Brandt, C., Dollfus, H., and Moulin, B. (2011). Bardet-Biedl syndrome: a study of the renal and cardiovascular phenotypes in a French cohort. Clin. J. Am. Soc. Nephrol. *6*, 22–29.

Jin, H., White, S.R., Shida, T., Schulz, S., Aguiar, M., Gygi, S.P., Bazan, J.F., and Nachury, M.V. (2010). The conserved Bardet-Biedl syndrome proteins assemble a coat that traffics membrane proteins to cilia. Cell *141*, 1208–1219.

Kanda, H., Tateya, S., Tamori, Y., Kotani, K., Hiasa, K., Kitazawa, R., Kitazawa, S., Miyachi, H., Maeda, S., Egashira, K., and Kasuga, M. (2006). MCP-1 contributes to macrophage infiltration into adipose tissue, insulin resistance, and hepatic steatosis in obesity. J. Clin. Invest. *116*, 1494–1505.

Kast-Woelbern, H.R., Dana, S.L., Cesario, R.M., Sun, L., de Grandpre, L.Y., Brooks, M.E., Osburn, D.L., Reifel-Miller, A., Klausing, K., and Leibowitz, M.D. (2004). Rosiglitazone induction of Insig-1 in white adipose tissue reveals a novel interplay of peroxisome proliferator-activated receptor gamma and sterol regulatory element-binding protein in the regulation of adipogenesis. J. Biol. Chem. *279*, 23908–23915.

Kohlroser, J., Mathai, J., Reichheld, J., Banner, B.F., and Bonkovsky, H.L. (2000). Hepatotoxicity due to troglitazone: report of two cases and review of adverse events reported to the United States Food and Drug Administration. Am. J. Gastroenterol. *95*, 272–276.

Laudes, M. (2011). Role of WNT signalling in the determination of human mesenchymal stem cells into preadipocytes. J. Mol. Endocrinol. *46*, R65–R72.

Le Lay, S., Krief, S., Farnier, C., Lefrère, I., Le Liepvre, X., Bazin, R., Ferré, P., and Dugail, I. (2001). Cholesterol, a cell size-dependent signal that regulates glucose metabolism and gene expression in adipocytes. J. Biol. Chem. *276*, 16904–16910.

MacKellar, J., Cushman, S.W., and Periwal, V. (2009). Differential effects of thiazolidinediones on adipocyte growth and recruitment in Zucker fatty rats. PLoS ONE *4*, e8196.

Mantovani, A., Sica, A., Sozzani, S., Allavena, P., Vecchi, A., and Locati, M. (2004). The chemokine system in diverse forms of macrophage activation and polarization. Trends Immunol. *25*, 677–686.

Marion, V., Schlicht, D., Mockel, A., Caillard, S., Imhoff, O., Stoetzel, C., van Dijk, P., Brandt, C., Moulin, B., and Dollfus, H. (2011). Bardet-Biedl syndrome highlights the major role of the primary cilium in efficient water reabsorption. Kidney Int. *79*, 1013–1025.

Marion, V., Stoetzel, C., Schlicht, D., Messaddeq, N., Koch, M., Flori, E., Danse, J.M., Mandel, J.L., and Dollfus, H. (2009). Transient ciliogenesis involving Bardet-Biedl syndrome proteins is a fundamental characteristic of adipogenic differentiation. Proc. Natl. Acad. Sci. USA *106*, 1820–1825.

Marion, V., Stutzmann, F., Gérard, M., De Melo, C., Schaefer, E., Claussmann, A., Hellé, S., Delague, V., Souied, E., Barrey, C., et al. (2012). Exome sequencing identifies mutations in LZTFL1, a BBSome and smoothened trafficking regulator, in a family with Bardet—Biedl syndrome with situs inversus and insertional polydactyly. J. Med. Genet. *49*, 317–321.

Mockel, A., Perdomo, Y., Stutzmann, F., Letsch, J., Marion, V., and Dollfus, H. (2011). Retinal dystrophy in Bardet-Biedl syndrome and related syndromic ciliopathies. Prog. Retin. Eye Res. *30*, 258–274.

Mok, C.A., Héon, E., and Zhen, M. (2010). Ciliary dysfunction and obesity. Clin. Genet. *77*, 18–27.

Mueller, W.M., Gregoire, F.M., Stanhope, K.L., Mobbs, C.V., Mizuno, T.M., Warden, C.H., Stern, J.S., and Havel, P.J. (1998). Evidence that glucose metabolism regulates leptin secretion from cultured rat adipocytes. Endocrinology *139*, 551–558.

Muruganandan, S., Roman, A.A., and Sinal, C.J. (2009). Adipocyte differentiation of bone marrow-derived mesenchymal stem cells: cross talk with the osteoblastogenic program. Cell. Mol. Life Sci. *66*, 236–253.

Nachury, M.V., Loktev, A.V., Zhang, Q., Westlake, C.J., Peränen, J., Merdes, A., Slusarski, D.C., Scheller, R.H., Bazan, J.F., Sheffield, V.C., and Jackson, P.K. (2007). A core complex of BBS proteins cooperates with the GTPase Rab8 to promote ciliary membrane biogenesis. Cell *129*, 1201–1213.

Novarino, G., Akizu, N., and Gleeson, J.G. (2011). Modeling human disease in humans: the ciliopathies. Cell *147*, 70–79.

Qiu, N., Cao, L., David, V., Quarles, L.D., and Xiao, Z. (2010). Kif3a deficiency reverses the skeletal abnormalities in Pkd1 deficient mice by restoring the balance between osteogenesis and adipogenesis. PLoS ONE *5*, e15240.

Rahmouni, K., Fath, M.A., Seo, S., Thedens, D.R., Berry, C.J., Weiss, R., Nishimura, D.Y., and Sheffield, V.C. (2008a). Leptin resistance contributes to obesity and hypertension in mouse models of Bardet-Biedl syndrome. J. Clin. Invest. *118*, 1458–1467.

Rahmouni, K., Fath, M.A., Seo, S., Thedens, D.R., Berry, C.J., Weiss, R., Nishimura, D.Y., and Sheffield, V.C. (2008b). Leptin resistance contributes to obesity and hypertension in mouse models of Bardet-Biedl syndrome. J. Clin. Invest. *118*, 1458–1467.

Satir, P., Pedersen, L.B., and Christensen, S.T. (2010). The primary cilium at a glance. J. Cell Sci. *123*, 499–503.

Scheen, A.J. (2001). Thiazolidinediones and liver toxicity. Diabetes Metab. *27*, 305–313.

Sen Gupta, P., Prodromou, N.V., and Chapple, J.P. (2009). Can faulty antennae increase adiposity? The link between cilia proteins and obesity. J. Endocrinol. *203*, 327–336.

Seo, S., Baye, L.M., Schulz, N.P., Beck, J.S., Zhang, Q., Slusarski, D.C., and Sheffield, V.C. (2010). BBS6, BBS10, and BBS12 form a complex with CCT/TRiC family chaperonins and mediate BBSome assembly. Proc. Natl. Acad. Sci. USA *107*, 1488–1493.

Seo, S., Guo, D.F., Bugge, K., Morgan, D.A., Rahmouni, K., and Sheffield, V.C. (2009). Requirement of Bardet-Biedl syndrome proteins for leptin receptor signaling. Hum. Mol. Genet. *18*, 1323–1331.

Sheffield, V.C. (2010). The blind leading the obese: the molecular pathophysiology of a human obesity syndrome. Trans. Am. Clin. Climatol. Assoc. *121*, 172–181, discussion 181–172.

Shoelson, S.E., Lee, J., and Goldfine, A.B. (2006a). Inflammation and insulin resistance. J. Clin. Invest. *116*, 1793–1801.

Shoelson, S.E., Lee, J., and Goldfine, A.B. (2006b). Inflammation and insulin resistance. J. Clin. Invest. *116*, 1793–1801.

Slagman, A.C., Bock, C., Abdel-Aty, H., Vogt, B., Gebauer, F., Janelt, G., Wohlgemuth, F., Morgenstern, R., Yapici, G., Puppe, A., et al. (2011). Specific removal of C-reactive protein by apheresis in a porcine cardiac infarction model. Blood Purif. *31*, 9–17.

Spiegelman, B.M. (1998). PPAR-gamma: adipogenic regulator and thiazolidinedione receptor. Diabetes *47*, 507–514.

Suh, J.M., Gao, X., McKay, J., McKay, R., Salo, Z., and Graff, J.M. (2006). Hedgehog signaling plays a conserved role in inhibiting fat formation. Cell Metab. *3*, 25–34.

Taipaleenmäki, H., Abdallah, B.M., AlDahmash, A., Säämänen, A.M., and Kassem, M. (2011). Wnt signalling mediates the cross-talk between bone marrow derived pre-adipocytic and pre-osteoblastic cell populations. Exp. Cell Res. *317*, 745–756.

van Tienen, F.H., van der Kallen, C.J., Lindsey, P.J., Wanders, R.J., van Greevenbroek, M.M., and Smeets, H.J. (2011). Preadipocytes of type 2 diabetes subjects display an intrinsic gene expression profile of decreased differentiation capacity. Int J Obes (Lond) *35*, 1154–1164.

Warne, J.P., Alemi, F., Reed, A.S., Varonin, J.M., Chan, H., Piper, M.L., Mullin, M.E., Myers, M.G., Jr., Corvera, C.U., and Xu, A.W. (2011). Impairment of central leptin-mediated PI3K signaling manifested as hepatic steatosis independent of hyperphagia and obesity. Cell Metab. *14*, 791–803.

Webb, M.P., Dicks, E.L., Green, J.S., Moore, S.J., Warden, G.M., Gamberg, J.S., Davidson, W.S., Young, T.L., and Parfrey, P.S. (2009). Autosomal recessive Bardet-Biedl syndrome: first-degree relatives have no predisposition to metabolic and renal disorders. Kidney Int. *76*, 215–223.

Weyer, C., Bogardus, C., Mott, D.M., and Pratley, R.E. (1999). The natural history of insulin secretory dysfunction and insulin resistance in the pathogenesis of type 2 diabetes mellitus. J. Clin. Invest. *104*, 787–794.

Xu, H., Barnes, G.T., Yang, Q., Tan, G., Yang, D., Chou, C.J., Sole, J., Nichols, A., Ross, J.S., Tartaglia, L.A., and Chen, H. (2003). Chronic inflammation in fat plays a crucial role in the development of obesity-related insulin resistance. J. Clin. Invest. *112*, 1821–1830.

Yokoi, T. (2010). Troglitazone. Handb. Exp. Pharmacol. 419–435.

Zaghloul, N.A., and Katsanis, N. (2009). Mechanistic insights into Bardet-Biedl syndrome, a model ciliopathy. J. Clin. Invest. *119*, 428–437.